

# A POLYTROPIC MODEL OF AN ACCRETION DISK, A BOUNDARY LAYER, AND A STAR

BOHDAN PACZYŃSKI

Princeton University Observatory, Peyton Hall, Princeton, NJ 08544

Received 1990 June 7; accepted 1990 September 19

## ABSTRACT

A model of a thin polytropic disk accreting onto a polytropic star through a polytropic boundary layer is presented. No a priori distinction is made in the manner various parts of the system are treated. A one-parameter series of models is calculated, with the stellar angular velocity varying from small to somewhat supercritical values along the series. All subcritical models accrete mass as well as angular momentum. For the most supercritical models accretion of mass is accompanied by the loss of angular momentum from the star to the disk, mediated by the viscous stresses. No termination of the series is noticed near the critical rotation rate. If anything, the supercritical models are simpler and easier to calculate than the models of disk accretion onto a slowly rotating star.

The “no torque boundary condition” arises naturally in the accretion onto a star with a subcritical rotation. There is no such condition for a star with a supercritical rotation, as angular velocity decreases monotonically with radius throughout the whole disk-star system.

*Subject headings:* hydrodynamics — stars: accretion — stars: binaries

## 1. INTRODUCTION

Disk accretion onto compact objects was a subject of many studies following the pioneering work of Shakura & Sunyaev (1973) and Lynden-Bell & Pringle (1974). It is believed that within a disk angular momentum is transferred outward through some unknown viscous process. As a result the matter spirals inward, and it ultimately accretes onto the central object. Even though the same matter is first part of the disk, then part of the boundary layer, and finally becomes part of the star, it is customary to describe the matter differently in these three environments (Pringle 1981, and references therein). One of the aims of this paper is to develop a simple polytropic model within which the whole system is treated in the same manner.

Accretion of matter with angular momentum spins up the central object. After accreting a finite amount of matter, typically after doubling its mass, the central object is spun up to the “break-up” rotation. It is commonly believed that once this happens further accretion becomes either impossible or cannot proceed without ejection of some mass and angular momentum (see Shu et al. 1988, and references therein). The second goal of this paper is to investigate the structure of the disk–boundary layer–star system when the so-called “break-up” condition develops, in order to find out if further accretion is indeed made difficult or impossible. According to Ghosh & Lamb (1979) and Pringle (1989), accretion may continue even near the “break up.”

## 2. MODEL

### 2.1. Outline

We are considering a model of a differentially rotating star that accretes matter from a disk. We assume hydrostatic equilibrium of the whole system, and we ignore all thermal processes by assuming a polytropic equation of state. The stellar mass increases on a time scale many orders of magnitude longer than the rotation period. We adopt a cylindrical coordinate system, in which  $r$  is the distance from the rotation axis and  $z$  is the distance from the equatorial plane (see Fig. 1).

In principle, the Poisson equation for the self-gravitating star should be solved to obtain a fully self-consistent model. This would significantly increase the complexity of calculations. Instead, gravitational potential of a point mass is adopted:

$$\Psi = -\frac{GM}{R} = -\frac{GM}{(r^2 + z^2)^{1/2}}, \quad (1)$$

where  $M$  is the stellar mass. This assumption makes it easier to concentrate on the main issue of this paper: the structure of the outer parts of the star, the boundary layer, and the inner parts of the disk.

We adopt a polytropic equation of state, with the pressure given as

$$P = K\rho^{1+1/n}, \quad (2)$$

where  $K$  and  $n$  are the two constants. This implies that angular velocity is constant on cylinders,  $\Omega = \Omega(r)$  (Tassoul 1978, p. 79). The same equation (2) holds for the whole system.

The whole star-disk system is divided into two parts, with the boundary between them located within the star, at some cylindrical transition radius  $r_{tr}$ . Almost all mass is expected to be at  $0 \leq r \leq r_{tr}$ , within the main body of the star, which is expected to rotate almost rigidly. This part of the system will be referred to as the “star.” The outer parts of the star, the boundary layer, and the accretion disk, located between  $r_{tr}$  and  $r_{out}$ , will be referred to as “disk-star.” The disk-star is expected to be in a steady state, with a constant rate of mass and angular momentum flow,  $\dot{M}$  and  $\dot{J}$ , between  $r_{out}$  and  $r_{tr}$ . The disk is thin and Keplerian at  $r_{out}$ , while the viscosity enforces almost rigid body rotation near  $r_{tr}$ .

On a very long accretion time scale,  $\tau_{accr}$ , the mass and angular momentum of the accreting star increase at the rates  $\dot{M}$  and  $\dot{J}$ . The total stellar mass  $M$  and its angular velocity  $\Omega_s$  change on this time scale. Gravitational potential (eq. [1]) and the assumption of the solid-body rotation allow calculation of the shape of stellar surface. In fact, this can be done analytically for  $0 \leq r \leq r_{tr}$ .

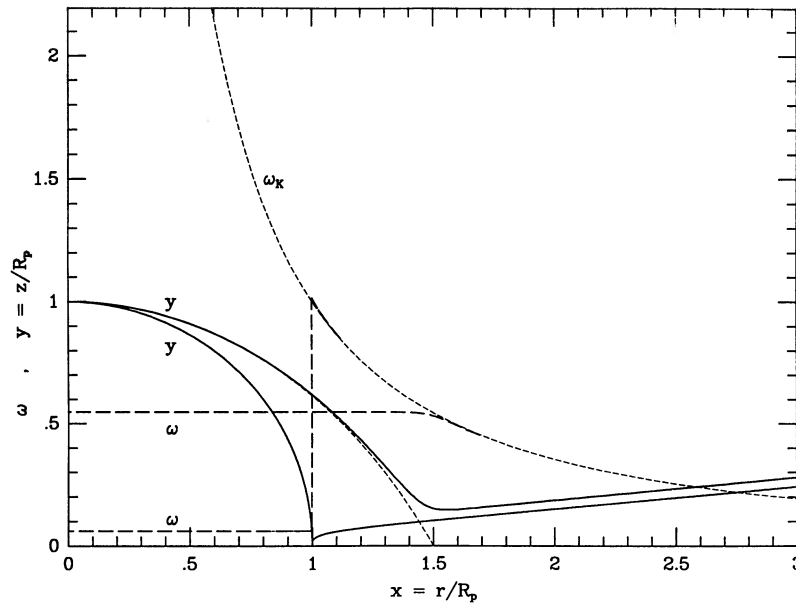


FIG. 1.—Meridional cross section of a star accreting matter from a thin disk. The rotation axis coincides with the  $z$ -axis, and the  $r$ -axis is in the equatorial plane. The surface of the star and the disk are shown with solid lines for model 1 (slowly rotating star, accreting mass, and angular momentum), and model 13 (rapidly rotating star, accreting mass, but no angular momentum). The variation of their angular velocity with radius is shown by long-dashed lines. Some parameters of the models are given in Table 1. One of the short-dashed lines shows the variation of Keplerian angular velocity with radius, and it is labeled “ $\omega_K$ .” The other short-dashed line shows the surface of an isolated star rotating with the critical angular velocity,  $\Omega_{cr} = (GM)^{1/2}/(1.5R_p)^{3/2}$ , where  $R_p$  is the polar radius of the star. This star has a cusp at its equator.

The time it takes matter to flow from  $r_{out}$  to  $r_{tr}$  is many orders of magnitude shorter than  $\tau_{accr}$ , and therefore the disk-star is assumed to be in a steady state accretion. Its structure is described by two ordinary differential equations: the equation of hydrostatic equilibrium, and the equation of angular momentum balance; these equations are derived in the following subsections. They have to be solved numerically as a boundary value problem in the region:  $r_{tr} \leq r \leq r_{out}$ .

To make the accretion possible viscous momentum transfer is calculated within the “ $\alpha$  disk model” convention. The same formula for viscosity is used throughout the whole disk-star system, and the two differential equations are identical all the way from  $r_{tr}$  to  $r_{out}$ . No distinction is made between the outer parts of the star, the boundary layer, and the disk. Once the solution of the equations is calculated such a distinction can be made, if it is desirable.

## 2.2. Hydrostatic Equilibrium

A differentially rotating star and disk are kept in a hydrostatic equilibrium by the balance between the gravitational acceleration, centrifugal acceleration, and the pressure gradient. The balance of these forces at the surface can be written in the following form:

$$r\Omega^2 = \left( \frac{\partial \Psi}{\partial r} \right)_z + \left( \frac{\partial \Psi}{\partial z} \right)_r \frac{dz_0}{dr}, \quad (3)$$

where  $z_0(r)$  is the variation of  $z$  with  $r$  along the surface. For the potential given with the equation (1) the equation of hydrostatic equilibrium may be written as

$$\frac{z_0 dz_0}{r dr} = \frac{R^3 \Omega^2}{GM} - 1 = \frac{(r^2 + z_0^2)^{3/2} \Omega^2}{GM} - 1. \quad (4)$$

This is the first equation relating the two unknown functions:  $z_0(r)$  and  $\Omega(r)$ .

## 2.3. Angular Momentum Balance

The equation of angular momentum balance in a steady state accretion disk may be written as (Lynden-Bell & Pringle 1974)

$$\dot{M} \frac{dj}{dr} - \frac{dg}{dr} = 0, \quad (5)$$

where

$$j(r) = r^2 \Omega(r) \quad (6)$$

is the specific angular momentum of matter, and  $g$  is the torque due to viscous stresses. This equation may be integrated to obtain

$$g = g_0 + \dot{M}(j - j_0) = \dot{M}j - (\dot{M}j_0 - g_0) = \dot{M}j - \dot{J}, \quad (7a)$$

where

$$\dot{M} = \text{const.}, \quad \dot{J} \equiv \dot{M}j - g = \text{const.}, \quad (7b)$$

and  $\dot{M}$  and  $\dot{J}$  are the two constants of the flow, viz., the accretion rates of mass and angular momentum.

The torque  $g(r)$  acting between the two adjacent cylinders of a differentially rotating object is given as

$$g = 2\pi r^3 \left( -\frac{d\Omega}{dr} \right) \int_{-z_0}^{z_0} \eta dz \quad (8)$$

(see Pringle 1981). If  $d\Omega/dr = 0$  at some radius  $r = r_0$ , then the corresponding torque vanishes,  $g_0 = 0$ , and a no-torque boundary condition may be applied there. This is the type of solution expected when slowly rotating star accretes from a thin disk.

The accretion is made possible by viscosity. We adopt the following formula for the dynamical viscosity  $\eta$ :

$$\eta = \alpha \rho_0 v_{s,0} z_0, \quad 0 < \alpha < 1, \quad (9)$$

where  $\alpha$  is a dimensionless constant,  $\rho_0$  is the density in the equatorial plane, and  $v_{s,0}$  is the speed of sound in the equatorial plane, given as

$$v_{s,0}^2 = \left( \frac{dP}{d\rho} \right)_{z=0} = \frac{n}{n+1} K \rho_0^{1/n}. \quad (10)$$

In a thin disk the equation of hydrostatic equilibrium in the  $z$ -direction is

$$\frac{1}{\rho} \frac{\partial P}{\partial r} \approx - \frac{GM}{r^3} z, \quad \frac{z}{r} \ll 1. \quad (11)$$

Combining equations (2) and (11) we obtain the distribution of density with a distance from the equatorial plane:

$$\rho = \rho_0 \left( 1 - \frac{z^2}{z_0^2} \right)^n, \quad \rho_0 = \left[ \frac{2GM}{(n+1)Kr^3} \right]^n z_0^{2n}. \quad (12)$$

Combining equations (10) and (12), the speed of sound in the equatorial plane may be written as

$$v_{s,0} = \left( \frac{2}{n} GM \right)^{1/2} \frac{z_0}{r^{1.5}}. \quad (13)$$

Finally, the dynamical viscosity as defined by equation (9) becomes

$$\eta = \left[ \alpha \frac{(GM)^{n+0.5}}{K^n} \right] \frac{z_0^{2n+2}}{r^{3n+1.5}}, \quad (14)$$

where we neglected a dimensionless term  $(2/n)^{1/2} [2/(n+1)]^n$ , since it is of order unity ( $=0.826$  for  $n=1.5$ ).

Now we may combine equations (8) and (14) to express the torque as

$$g = \left[ 4\pi\alpha \frac{(GM)^{n+0.5}}{K^n} \right] \frac{z_0^{2n+3}}{r^{3n-1.5}} \left( -\frac{d\Omega}{dr} \right). \quad (15)$$

This equation has been derived for a thin disk. However, the  $\alpha$  viscosity concept is entirely ad hoc, and it is used as a convenient way to parametrize our lack of understanding of the true physical processes. In this paper we shall use the same equation (15) to describe viscous stresses not only in the disk, but also within the star and within the boundary layer. This implies that the viscosity inside the star is very large, since  $z_0/r$  is large there. This is likely to enforce a near rigid body rotation for the star, in agreement with a standard approximation.

The equation (15) may be rewritten in a slightly different form, taking into account equations (6) and (7):

$$\left[ 4\pi\alpha \frac{(GM)^{n+0.5}}{K^n} \right] \frac{d\Omega}{dr} = \frac{r^{3n-1.5}}{z_0^{2n+3}} (J - \dot{M} r^2 \Omega). \quad (16)$$

This is the equation of angular momentum balance, and the second relation between the two unknown functions:  $z_0(r)$  and  $\Omega_0(r)$ .

#### 2.4. Outer Boundary Condition

At the outer boundary, at some large radius  $r_{\text{out}}$ , the derivative of angular velocity is Keplerian:

$$\left( \frac{d\Omega}{dr} \right)_{r_{\text{out}}} = \left( \frac{d\Omega_K}{dr} \right)_{r_{\text{out}}} = -\frac{3}{2} \frac{(GM)^{1/2}}{r_{\text{out}}^{5/2}}. \quad (17)$$

It is assumed that there is a steady mass and angular momentum flow,  $\dot{M}$  and  $J$ , across the outer boundary.

#### 2.5. Inner Boundary Condition

At the inner boundary we require

$$\Omega(r_{\text{tr}}) = \Omega_s, \quad (18)$$

where  $\Omega_s$  is the angular velocity of the accreting star, a free parameter of our problem. It is assumed that there is a steady mass and angular momentum flow,  $\dot{M}$  and  $J$ , across the inner boundary.

#### 2.6. Accreting Star

The accreting star is not in a steady state as mass and angular momentum accumulate within it. Therefore, the equation (16) is not applicable. However, the torque given with the equation (15) enforces an almost rigid body rotation for  $r \leq r_{\text{tr}}$ . Therefore, the equation of hydrostatic equilibrium (4) is supplemented by the assumption  $\Omega = \Omega_s = \text{constant}$ , sufficient to calculate the shape of the stellar surface,  $z_0(r)$ . Equation (4) may be rewritten as

$$\frac{d(R^2)}{d(r^2)} = R^3 \frac{\Omega_s^2}{GM}, \quad (19)$$

where  $R^2 = r^2 + z_0^2$ ,  $0 \leq r \leq r_{\text{tr}}$ , and  $\Omega_s^2/GM = \text{constant}$ . This may be integrated to obtain

$$z_0(r) = \left[ \left( \frac{1}{R_p} - \frac{\Omega_s^2 r^2}{2GM} \right)^{-2} - r^2 \right]^{1/2}, \quad 0 \leq r \leq r_{\text{tr}}, \quad (20)$$

where  $R_p = z_0(0)$  is the polar radius of the star.

If this was an isolated star rotating as a rigid body, the solution (20) could be extended all the way to the stellar equator at  $r = R_e$ , where  $z_0(R_e) = 0$ . The polar and the equatorial radii of an isolated star are related by the equation:

$$\frac{R_e}{R_p} - \frac{\Omega_s^2 R_e^3}{2GM} = 1, \quad 1 \leq \frac{R_e}{R_p} \leq 1.5, \quad (21)$$

which holds for stellar rotation rates in the range

$$0 \leq \Omega_s^2 \leq \Omega_{\text{cr}}^2 = \frac{GM}{R_e^3}, \quad \Omega_{\text{cr}}^2 = \frac{GM}{(1.5R_p)^3}. \quad (22)$$

A nonrotating star is spherical, and  $R_e = R_p$ . At the critical rotation rate,  $\Omega_s = \Omega_{\text{cr}}$ , the equatorial radius is 50% larger than the polar radius,  $R_e = 1.5R_p$ , and a cusp forms at the equator. An isolated star cannot rotate any faster.

Some models to be presented in this paper rotate somewhat faster than the “break up,” i.e., their angular velocity  $\Omega_s$  is somewhat larger than  $\Omega_{\text{cr}}$ . An isolated star cannot spin that fast, and the stellar surface as calculated with the equation (20) cannot be extended all the way to equator, but it can always extend out to  $r_{\text{tr}}$ , the boundary between the star and the disk-star system.

#### 2.7. Dimensionless Equations

It is convenient to write the equations in dimensionless form. All lengths can be expressed in units of some characteristic radius  $R_*$ , to be defined later. The following notation will be adopted from now on:

$$x = \frac{r}{R_*}, \quad x_e = \frac{R_e}{R_*}, \quad (23a)$$

$$y = \frac{z_0}{R_*}, \quad y_p = \frac{R_p}{R_*}, \quad (23b)$$

$$\omega^2 = \Omega^2 \frac{R_*^3}{GM}, \quad \omega_s^2 = \Omega_s^2 \frac{R_*^3}{GM}, \quad \omega_{\text{cr}}^2 = \Omega_{\text{cr}}^2 \frac{R_*^3}{GM}. \quad (23c)$$

All numerical computations are done for one value of the polytropic index only:  $n = 1.5$ . Therefore, all the equations will now be written for  $n = 1.5$  only. Using the dimensionless variables, the equations (4) and (16) may be written as

$$\frac{y}{x} \frac{dy}{dx} = \omega^2(x^2 + y^2)^{3/2} - 1, \quad x_{\text{tr}} \leq x \leq x_{\text{out}}, \quad (24a)$$

(hydrostatic equilibrium),

$$\frac{d\omega}{dx} = \frac{1}{a} \frac{x^3}{y^6} (j_* - \omega x^2), \quad x_{\text{tr}} \leq x \leq x_{\text{out}}, \quad (24b)$$

(momentum balance),

where the two constants are

$$a \equiv 4\pi\alpha \frac{G^2 M^2}{\dot{M} K^{1.5}} = \text{const.}, \quad (25a)$$

$$j_* \equiv \frac{j}{\dot{M}(GMR_*)^{1/2}} = \text{const.} \quad (25b)$$

The boundary conditions are given as

$$\omega = \omega_s, \quad x = x_{\text{tr}}, \quad (26a)$$

(inner boundary),

$$\frac{d\omega}{dx} = \frac{d\omega_K}{dx} = -1.5x_{\text{out}}^{-2.5}, \quad x = x_{\text{out}}, \quad (26b)$$

(outer boundary),

The shape of the stellar surface is given by the formula

$$y = [(y_p^{-1} - 0.5\omega_s^2 x^2)^{-2} - x^2]^{1/2}, \quad 0 \leq x \leq x_{\text{tr}}. \quad (27)$$

The surface described with this equation can be extended all the way to the equator of an isolated star rotating as a rigid body, provided its rotation is subcritical:

$$0 \leq \omega_s \leq \omega_{\text{cr}} \equiv (1.5y_p)^{-1.5}, \quad (28)$$

(isolated star),

(see eq. [22]). There is no a priori reason why the accreting star should not rotate faster than  $\omega_{\text{cr}}$ , so the range given above does not apply to our models. Still it is convenient to express the angular velocity of a star as  $\omega_s/\omega_{\text{cr}}$ , or  $\Omega_s/\Omega_{\text{cr}}$ .

### 2.8. Dimensionless Constants

The dimensionless constant  $a$  defined by equation (25a) has a simple physical meaning. Let us consider the star to be a self-gravitating  $n = 1.5$  polytrope with the polytropic constant  $K$ . The mass-radius relation for a spherical star is given by Chandrasekhar (1939) as

$$K = 0.4242GM^{1/3}R, \quad (29)$$

The same relation must hold for some effective radius of a rotating star,  $R_*$ . In order to be more precise we would have to solve the Poisson equation for the rotating star. Instead, we combine the equations (25a) and (29) to write an approximate relation:

$$a \approx 4\pi\alpha \left( \frac{M}{\dot{M}} \right) \left( \frac{GM}{R_*^3} \right)^{1/2} \approx 8\pi^2\alpha \frac{\tau_{\text{accret}}}{P_{\text{rot}}}, \quad (30)$$

where  $\tau_{\text{accret}}$  is the accretion time scale and  $P_{\text{rot}}$  is the shortest possible rotation period for the accreting star. For a pre-main-

sequence star we may expect  $\tau_{\text{accret}} \approx 10^6$  yr, and  $P_{\text{rot}} \approx 1$  hr, so  $a \approx 10^{1.2}\alpha$ . For an accreting white dwarf we may have  $a \approx 10^{1.5}\alpha$ . It is clear that  $a \gg 1$  is a good guess. Throughout our numerical computations  $a = 10^6$  is adopted. In the next section we show that the disk thickness can be estimated to be  $(z_0/r)_{\text{disk}} \approx a^{-1/6}$ . Our choice of  $a$  implies  $(z_0/r)_{\text{disk}} \approx 0.1$ , so the disk is thin, but not very thin. Numerical computations become somewhat more troublesome when a much larger value of the constant  $a$ , i.e., a much thinner disk, is chosen.

The constant  $j_*$  defined by equation (25b) is the dimensionless angular momentum accreted by the star. It is convenient to define its critical value as

$$j_{\text{cr}} \equiv \dot{M}(1.5R_p)^2\Omega_{\text{cr}} = \dot{M}(1.5GMR_p)^{1/2}, \\ j_{*,\text{cr}} \equiv (1.5y_p)^2\omega_{\text{cr}} = (1.5y_p)^{1/2}, \quad (31)$$

and to use the ratio  $j/j_{\text{cr}}$  or  $j_*/j_{*,\text{cr}}$  to describe the models.

### 3. SOLUTION

The following method should work for any model described by equations (24a)–(24b), but it works well only for models with a star which rotates close to the “break up.” Nevertheless, it offers a convenient way of analyzing the problem.

All computations were done for one polytropic index,  $n = 1.5$ , which corresponds to the adiabatic relation for a perfect, nonrelativistic gas, and  $a = 10^6$  was adopted in all models. There are three more constants in the equations (24a)–(24b) and in the boundary conditions (26a)–(26b). These are the accretion rate of angular momentum  $j_*$ , the stellar angular velocity  $\omega_s$ , and the polar radius  $y_p$ . The polar radius comes only as a scaling factor, provided the other two parameters are expressed as  $j_*/j_{*,\text{cr}}$  and  $\omega_s/\omega_{\text{cr}}$  (see eqs. [28], [31]). The following analysis will demonstrate that if  $\omega_s/\omega_{\text{cr}}$  is chosen to be a free parameter, then  $j_*/j_{*,\text{cr}}$  becomes an eigenvalue of the problem. Therefore, apart from scaling, there is only one parameter that varies along the sequence of models.

Let us consider the following procedure. The polar radius of the accreting star is fixed as  $y_p$ , and the transition radius is fixed as  $x_{\text{tr}} = 0.8y_p$ . The stellar thickness at  $x_{\text{tr}}$  can be calculated with equation (27) as  $y_s(\omega_s)$ . A solution of equations (24a)–(24b) between  $x_{\text{tr}}$  and  $x_{\text{out}} \gg x_{\text{tr}}$  depends on two parameters:  $j_*$ , which appears in equation (24b), and  $\omega_s$ , which appears in the boundary condition (26a). The thickness of the disk-star at  $x_{\text{tr}}$  is obtained as  $y_{\text{ds}}(\omega_s, j_*)$ . Of course, we have a matching condition between the star and the disk star, which requires that  $y_s(\omega_s) = y_{\text{ds}}(\omega_s, j_*)$ . This is possible for one value of  $j_*$  only, and so we find  $j_* = j_*(\omega_s)$ .

In practice, two somewhat different procedures were needed to calculate the models.

In the first procedure the solution of equations (24a)–(24b) is calculated numerically as a boundary value problem, using a relaxation method. This requires an initial guess for the values of all variables between the inner and the outer boundary. We begin assuming Keplerian angular velocity, i.e.,  $\omega \approx x^{-1.5}$ , which may be differentiated to obtain  $d\omega/dr = -1.5x^{-2.5}$ . Now equation (24b) may be used to estimate the variation of  $y(x)$ :

$$y \approx (1.5a)^{-1/6} x (1 - j_* x^{-1/2})^{1/6}. \quad (32)$$

The approximation provided by this equation was good enough as the initial guess, and the relaxation method converged in  $\sim 10$  iterations, using  $\sim 1000$  mesh points spread uniformly in  $\log x$  between  $x_{\text{tr}} = 0.8$  and  $x_{\text{out}} = 10$ . The polar



radius of the star was chosen as a unit of length, i.e.,  $y_p = 1$  was adopted.

It was easy to find models rotating close to “break up” velocity, with the angular velocity  $\omega$  decreasing monotonically between  $x_{tr}$  and  $x_{out}$ . When stellar rotation was reduced below the “break-up” rate, a local maximum appeared in the angular velocity between the rigidly rotating star and the Keplerian disk, and the “no torque” condition within the boundary layer came out automatically as a solution of equations (24a)–(24b). However, as models with lower angular velocity of the star were calculated, the convergence of the relaxation method slowed down. It was necessary to redistribute the mesh points so that no variable was changing by more than 0.5% of its value between any two adjacent mesh points. A solution obtained for one model had to be used as the initial guess for the next one, with a slightly smaller value of  $\omega_s$ . Still the relaxation technique that covered the whole disk-star system between the rigidly rotating star at  $x_{tr}$  and the Keplerian outer boundary at  $x_{out}$  became very inefficient when the stellar rotation rate  $\omega_s$  became significantly subcritical.

Another method was found to work well for accretion onto a slowly rotating star. The numerical problems with the first series of models were encountered only when the distribution of angular velocity had a well-developed maximum. For these models the matching point between the star and the disk may be moved to the position of that maximum, and the new inner boundary condition for the disk may be written as

$$\left(\frac{d\omega}{dx}\right)_{x_{in}} = 0, \quad x_{in} = 1. \quad (33)$$

This is the standard “no torque” condition commonly used at the disk-star boundary. Now equations (24a)–(24b) were solved numerically with a relaxation method for  $x_{in} \leq x \leq x_{out}$ , and  $j_*$  was the only parameter that varied from one model to another. In particular, the disk thickness at  $x_{in}$  was calculated as  $y_d = y_d(j_*)$ .

The calculation of the stellar structure was somewhat more complicated, since it was described with three parameters:  $\omega_s$ ,  $y_p$ , and  $j_*$ . The following procedure was found to work. First, the polar radius  $y_p$  and the stellar rotation rate  $\omega_s$  were selected, and equation (27) was used to calculate the shape of stellar surface for  $0 \leq x \leq x_{tr} = 0.8$ , and in particular to calculate stellar thickness at  $x = x_{tr}$ . This part of the solution did not depend on  $j_*$ . Next, equations (24a)–(24b) were integrated with the first order, fully implicit Runge-Kutta method between  $x = x_{tr} = 0.8$  and  $x = x_{in} = 1$ . The value of  $j_*$  adopted for this integration was the same as the one used for the disk. The stellar thickness  $y_s$  and the derivative of angular velocity  $\omega'_s \equiv (d\omega/dx)_{x=x_{in}}$  were calculated at  $x = x_{in}$  as a function of  $y_p$  and  $\omega_s$ . Next  $y_p$  and  $\omega_s$  were adjusted so as to satisfy the two conditions at  $x = x_{in}$ :  $\omega'_s(y_p, \omega_s) = 0$  and  $y_s(y_p, \omega_s) = y_d(j_*)$ . These two matching conditions gave  $y_p = y_p(j_*)$  and  $\omega_s = \omega_s(j_*)$ . This method worked well for any star with a rotational velocity that was below the “break up.”

#### 4. RESULTS

Many models of the disk-star system were calculated. Some parameters for 14 models are given in Table 1. The first seven models were computed with the interface between the star and the disk put at the radius where  $d\Omega/dr = 0$ , while the interface for the last seven models was at  $r/R_p = 0.8$ . There is some overlap between the two series of models, calculated with the somewhat different numerical techniques, as described in the

TABLE 1  
PARAMETERS FOR SELECTED MODELS

Model	$\tilde{J}/\tilde{J}_{cr}$	$\Omega_s/\Omega_{cr}$	$R_e/R_p$
1.....	1.8647	0.1111	1.0018
2.....	2.0014	0.8273	1.1571
3.....	2.0986	0.9468	1.2757
4.....	2.1621	0.9827	1.3595
5.....	2.1981	0.9942	1.4148
6.....	2.2126	0.9980	1.4521
7.....	2.1843	1.0010	...
8.....	2.2145	0.9991	1.4653
9.....	2.2045	1.0003	...
10.....	2.1311	1.0018	...
11.....	1.8371	1.0035	...
12.....	1.1023	1.0052	...
13.....	0.0000	1.0066	...
14.....	-1.8371	1.0081	...

previous section. The meridional cross section of the models, i.e., the variation of  $z_0(r)$  with  $r$ , is shown in Figures 2a and 3a for the two series of models, and the variation of their rotation rate with radius is shown in Figures 2b and 3b.

Models 1–6 and 8 are of the type that has been expected: the accreting star rotates with a subcritical angular velocity  $\Omega_s$ . The mass and angular momentum are accreted together, since  $\tilde{J}$  is positive. The disk-star system has the minimum thickness,  $z_{0,min}$ , close to the radius  $r = R_m$ , where the angular velocity reaches its maximum. While the accreting star is spun up by accretion,  $z_{0,min}$  increases, and the pressure at the boundary layer increases too.

The nonzero pressure at the equatorial plane at  $R_m$  makes it possible for the star to be spun up somewhat above the critical rate, and still accrete not only mass but also angular momentum: models 7 and 9–12 in Table 1 have  $\Omega_s > \Omega_{cr}$  and  $\tilde{J} > 0$ . An isolated star cannot rotate as a rigid body for  $\Omega_s > \Omega_{cr}$ .

If the star is spun up even more, up to  $\Omega_s = 1.0066\Omega_{cr}$ , the viscous torques transport outward just as much angular momentum as the accreting matter is bringing in, and  $\tilde{J} = 0$  (model 13 in Table 1). If the star rotates even faster, it can accrete matter but loses angular momentum, which is transported out from the star to the disk, since  $\tilde{J} < 0$  (model 14 in Table 1). This should not be surprising since disk accretion is made possible by the outward transport of angular momentum by viscosity, a common phenomenon in any accretion disk. Model 14 is doing just that not only for the disk, but also for the star.

#### 5. DISCUSSION

The main result of this paper is the demonstration that there is no limit to the amount of mass that can be accreted from a disk onto a star. All models can be arranged in a linear series with the dimensionless angular velocity of the star,  $\Omega_s/\Omega_{cr}$  (see eqs. [22], [28]), varying monotonically along that sequence. The dimensionless accretion rate of angular momentum,  $\tilde{J}/\tilde{J}_{cr}$  (see eq. [31]), changes sign when the rotation becomes somewhat supercritical, as shown in Table 1. As long as rotation is subcritical, the value of  $\tilde{J}/\tilde{J}_{cr}$  is almost constant (models 1–6 and 8). When the angular velocity of the star exceeds the critical value by just 0.5% (model 12), the value of  $\tilde{J}/\tilde{J}_{cr}$  drops dramatically and becomes negative for  $\Omega > 1.0066\Omega_{cr}$ . By the time  $\Omega_s/\Omega_{cr} = 1.008$  (model 14) the loss of angular momentum by the star becomes very efficient, since it is transferred to the disk through viscous stresses.

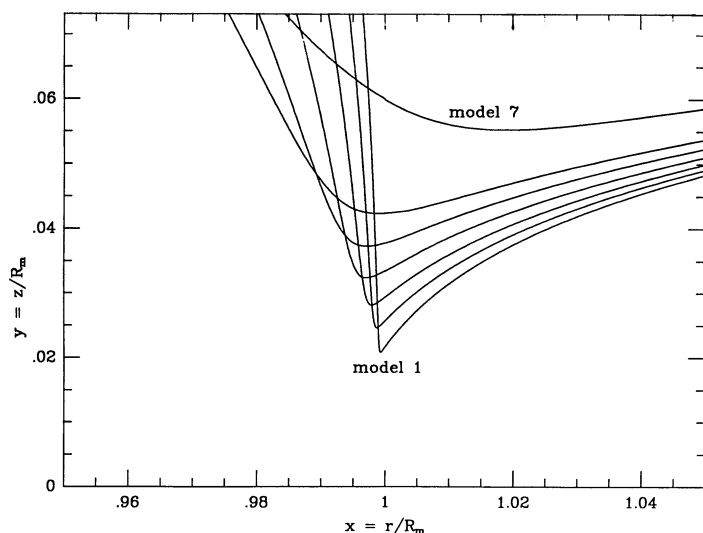


FIG. 2a

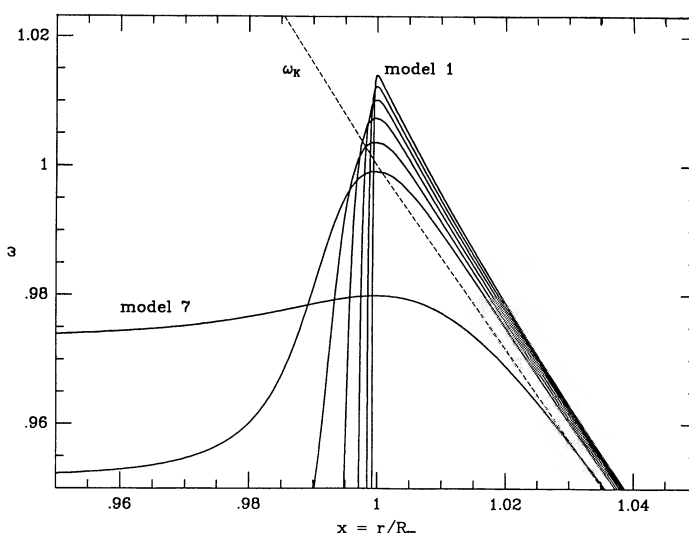


FIG. 2b

FIG. 2.—(a) A small region near the boundary layer is shown for models 1–7. The surface of the star–boundary layer–disk system is shown with solid lines. Model 7 rotates with a supercritical angular velocity. The unit length,  $R_m$ , corresponds to the radius at which angular velocity reaches the maximum, at which the “no torque boundary condition” can be applied. (b) The variation of angular velocity with radius is shown for models 1–7 by solid lines. The Keplerian angular velocity is shown with a broken line. The unit of length,  $R_m$ , corresponds to the radius at which angular velocity reaches its maximum, at which “no torque boundary condition” can be applied.

The star can accrete matter as long as the supply continues, even if the rotation is supercritical. The models presented here are very simple, but the result should be general. The structure of supercritical models is considerably simpler than the structure of slow rotators. The latter have a thin boundary layer with very large velocity gradients, as clearly shown in Figures 1 and 2b. These steep velocity gradients not only make the numerical computations somewhat difficult, but they may also lead to some instabilities. By contrast the structure of a rapidly rotating, accreting star is very simple, with a very gradual

transition between the disk and the star, as shown in Figures 3a and 3b (models 11–14).

When this project was almost completed, I learnt that Popham & Narayan (1991) reached very similar conclusions with a somewhat different model. The major difference is that some of their models developed supersonic radial infall, terminated by a shock wave. All models described in the present paper were assumed to be in a hydrostatic equilibrium, and the radial flow was assumed to be subsonic. Let us check the self-consistency of this assumption.

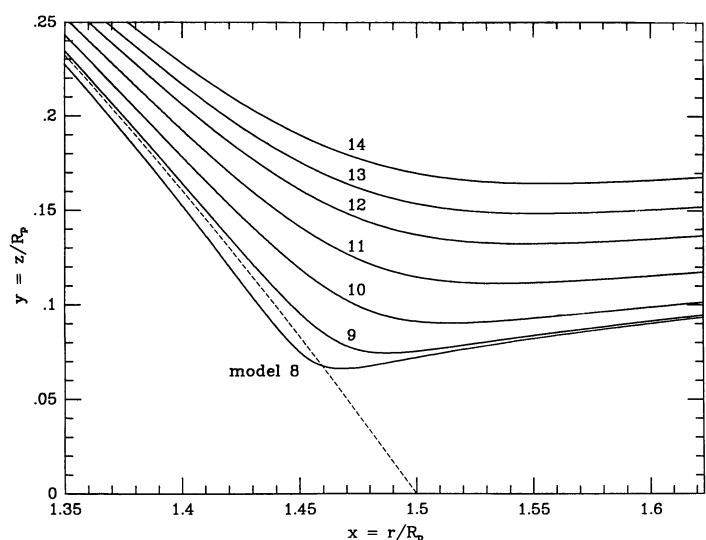


FIG. 3a

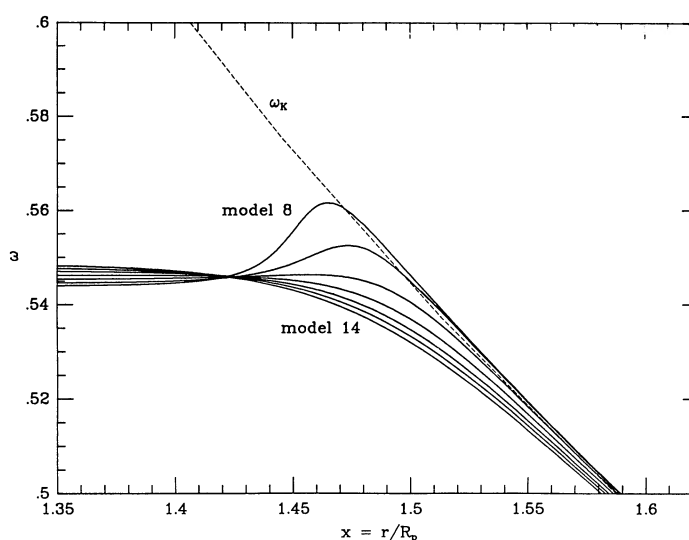


FIG. 3b

FIG. 3.—(a) A small region near the boundary layer is shown for models 8–14. The surface of the star–boundary layer–disk system is shown with solid lines. Models 9–14 rotate with supercritical angular velocity. Model 13 accretes matter but no angular momentum. Model 14 accretes matter and loses angular momentum to the disk through viscous stresses. The dashed line corresponds to the surface of an isolated star rotating with the critical angular velocity; it has a cusp at the equator. The unit of length is the polar radius of the star,  $R_p$ . (b) The variation of angular velocity with radius is shown for models 8–14 by solid lines. The Keplerian angular velocity is shown with a broken line. The unit of length is the polar radius of the star,  $R_p$ .

The radial velocity may be calculated as

$$v_r = \frac{\dot{M}}{2\pi r \Sigma}, \quad (34)$$

where

$$\begin{aligned} \Sigma &= \int_{-z_0}^{z_0} \rho dz = \rho_0 z_0 2 \int_0^1 (1 - u^2)^3 du \\ &= \frac{3\pi}{8} \rho_0 z_0 \approx 1.178 \rho_0 z_0, \end{aligned} \quad (35)$$

(see eq. [12]). Combining equations (13), (34), and (35), we may calculate the ratio of the radial velocity to the speed of sound as

$$\begin{aligned} \frac{v_r}{v_s} &= \left[ \frac{5}{4\pi^2} \left( \frac{5}{3} \right)^{1/2} \frac{\dot{M} K^{1.5}}{G^2 M^2} \right] \left( \frac{r}{z_0} \right)^5 \\ &= \left( \frac{5}{\pi^2} \right) \left( \frac{\alpha}{a} \right) \left( \frac{r}{z_0} \right)^5 \approx 2 \times 10^{-6} \alpha \left( \frac{r}{z_0} \right)^5, \end{aligned} \quad (36)$$

where  $a = 10^6$  and  $n = 1.5$  were adopted, and the definition (25a) was used in the transformation.

According to equation (36), the radial Mach number reaches maximum at the point where the disk-star system is the thin-

nest, i.e., close to  $r = R_m$  in Figure 2a. There is not much problem with the accretion onto a rapidly spinning star, since the ratio  $r/z_0$  is not very large there. However, there may be a problem at the boundary layer between the disk and a slowly rotating star. In the most extreme model (i.e., model 1), we have  $(z_0/r)_{\min} \approx 0.02$ , and therefore according to equation (36),  $(v_r/v_s)_{\max} \approx 600\alpha$ . The condition  $v_r/v_s \ll 1$  is satisfied provided  $\alpha \ll 0.001$ , i.e., if the viscosity is very small. If the viscosity is large, the flow may become supersonic, most easily when the accreting star rotates very slowly, and then the models presented in this paper break down.

If  $\alpha \approx 1$ , i.e., the viscosity is very high, then according to equation (36), we need  $(z_0/r)_{\max} < 0.07$  in order to have subsonic accretion ( $v_r/v_s < 1$ ) throughout the disk and the star. This is satisfied by the models 9–14 (see Fig. 3a). Once again the rapidly rotating models are the simplest: they remain in hydrostatic equilibrium even for the highest disk viscosity.

It is a pleasure to acknowledge that some programs used to calculate the model presented in this paper were tested by Ms. D. A. Daugherty as part of her Senior Project. I am indebted to Robert Popham and Ramesh Narayan, who kindly sent me the results of their work prior to publication. This project was partly supported by NSF grant AST 87-18432.

#### REFERENCES

- Chandrasekhar, S. 1939, *An Introduction to the Study of Stellar Structure* (Chicago: University of Chicago Press)  
 Ghosh, P., & Lamb, F. K. 1979, *ApJ*, 234, 296  
 Lynden-Bell, D., & Pringle, J. E. 1974, *MNRAS*, 168, 603  
 Popham, R., & Narayan, R. 1991, *ApJ*, 370, in press  
 Pringle, J. E. 1976, *MNRAS*, 177, 65  
 Pringle, J. E. 1981, *ARAA*, 19, 137  
 ———. 1989, *MNRAS*, 236, 107  
 Shakura, N. I., & Sunyaev, R. A. 1973, *A&A*, 24, 337  
 Shu, F. H., Lizang, S., Ruden, S. P., & Najita, J. 1988, *ApJ*, 328, L19  
 Tassoul, J.-L. 1978, *Theory of Rotating Stars* (Princeton: Princeton University Press)